Available online at www.sciencedirect.com
ScienceDirect
Polymer 48 (2007) 3982–3989
polymer
www.elsevier.com/locate/polymer

Characterization of poly(2-hydroxyethyl methacrylate-silica) hybrid materials with different silica contents

Shuxi Li [a], Apoorva Shah [b], Alex J. Hsieh [c], Ross Haghighat [b], S. Solomon Praveen [a], Indraneil Mukherjee [a], Elizabeth Wei [a], Zongtao Zhang [a,d], Yen Wei [a,*]

[a] *Department of Chemistry, The Center for Advanced Polymers and Materials Chemistry, Drexel University, 3141 Chestnut Street, Philadelphia, PA 19104, USA*
[b] *Triton Systems, Inc., Chelmsford, Massachusetts 01824, USA*
[c] *Army Research Laboratory, AMSRD-ARL-WM-MD, Aberdeen Proving Ground, MD 21005-5069, USA*
[d] *Department of Chemistry, Jilin University, Changchun 130023, PR China*

Received 30 January 2007; received in revised form 4 May 2007; accepted 9 May 2007
Available online 18 May 2007

Abstract

Poly(2-hydroxyethyl methacrylate-silica) hybrid materials with significantly lower volume shrinkage were synthesized by using acid-catalyzed sol–gel reactions of tetraethyl orthosilicate and free radical polymerization of 2-hydroxyethyl methacrylate (HEMA). The mechanical, thermal, and optical properties and internal porosities of the poly(HEMA-silica) hybrids with different silica contents (e.g., 15, 25 and 30 wt%) were evaluated with the use of nanoindentation, microscratch, thermogravimetric analysis, differential scanning calorimetry, dynamic mechanical analysis, UV–vis spectrophotometer and N_2 adsorption–desorption method. A silica percolation threshold was found at around 20–25 wt%, beyond which a marked increase in the poly(HEMA-silica) hybrid hardness and modulus was observed as compared to pure poly(HEMA). Nanoindentation and scratch testing measurements also for the first time were introduced in characterizing poly(HEMA-silica) hybrid materials.

Keywords: Poly(HEMA-silica) hybrid materials; Sol–gel synthesis; Nanoindentation

1. Introduction

Sol–gel technology is the most common route for the synthesis of inorganic–organic hybrid materials. A number of organic polymers have been incorporated into silica or other metal oxides (with or without covalent bonding) through the sol–gel procedure. Numerous articles, reviews and books have been published related to inorganic–organic hybrid materials [1–12]. There are several strategies in the synthesis of hybrid polymers via sol–gel techniques [13]. One of the strategies involves the simultaneous growth of the inorganic phase via acid- or base-catalyzed hydrolysis and condensation of alkoxysilane precursors and the polymer phase via free radical polymerization of vinyl monomers in a common solvent. This is followed by co-condensation of the two phases and slow removal of solvent to obtain the final hybrid nanocomposite materials. However, hybrids obtained from traditional sol–gel synthesis techniques have high volume shrinkage (e.g., 50–75%) [14], which is associated with the removal of large amounts of solvents and by-products from hydrolysis and condensation reactions (e.g., water and alcohol). As a result of high volume shrinkage, the final shape and dimension of the organic–inorganic hybrid monolith cannot be controlled. Furthermore, the stress induced by the volume shrinkage often causes the monolith to crack or break. These problems severely limit the fabrication of large, thick organic–inorganic hybrid objects via conventional casting methods.

In fact, the organic–inorganic hybrid materials with excellent properties have been demonstrated as a type of promising materials in many applications. One of challenges in non-blend

* Corresponding author. Tel.: +1 215 895 2650; fax: +1 215 895 1265.
E-mail address: weiyen@drexel.edu (Y. Wei).

0032-3861/$ - see front matter © 2007 Elsevier Ltd. All rights reserved.
doi:10.1016/j.polymer.2007.05.025

hybrid process is the volume shrinkage that comes from sol–gel process and polymerization of vinyl monomers. A lot of remarkable works and technologies have been done in different hybrid systems in order to overcome this problem. For instance, Yeh et al. [15] reported the effect of baking treatment and materials' composition on the properties of bulky PMMA-silica hybrid sol–gel materials with low volume shrinkage. Wang and coworkers [16] used $SiH(OC_2H_5)_3$ as a gel accelerant and got transparent noncracking, high-purity silica gel monoliths with a lower volume shrinkage. Frey and coworkers [17] synthesized bismethacrylate-based hybrid monomers with pendant, condensable alkoxysilane groups and then formed the inorganic networks by sol–gel condensation of the alkoxysilane groups in the presence of aqueous methacrylic acid. After photopolymerization, the organic–inorganic hybrid materials have low volume shrinkage in the range from 4.2% to 8.3%. Cho et al. [18] synthesized various structures of siloxane-containing epoxy compounds and polymerized these functional groups by rapid cationic photopolymerization to obtain transparent hybrid materials with low volume shrinkage. Rao et al. [19] reported that methyltrimethoxysilane was added in the sol–gel processing of silica aerogels. The volume shrinkage of the transparent aerogels reached <5%. Although it will be desirable to further reduce the volume shrinkage to values below 5% in the poly(HEMA-silica) system, but it should be noted that 5–10% volume shrinkage as reported has a remarkable improvement in comparison with 50–75% for typical sol–gel processing.

Synthesis and evaluation of poly(HEMA-silica) hybrid polymers have attracted tremendous research interest over the years [20,21]. Hajji et al. [22] studied the synthesis–morphology–mechanical property relationships of poly(HEMA-silica) nanocomposites using solid ^{29}Si nuclear magnetic resonance (NMR) spectroscopy, transmission electron microscopy (TEM), small-angle X-ray scattering (SAXS) and dynamic mechanical analysis (DMA) measurements. They also investigated the strength of poly(HEMA-silica) coating using bending tests [23]. Lin et al. [24] analyzed the chemical structure of poly(HEMA-silica) using solid ^{29}Si NMR, TEM and FESEM. In addition, viscosity, particle size distribution and structure of poly(HEMA-silica) during acid- and base-catalyzed sol–gel process were studied by Huang et al. [25] using cone/plate rheometer, DynaPro molecular sizing instrument, Oswald capillary viscometer, Fourier transform infrared (FTIR) spectrometer, differential scanning calorimetry (DSC), thermogravimetric analysis (TGA) and ultraviolet spectrophotometer. In the mean time, morphology controlled syntheses were developed by using polymerizable templates to form self-assembly of monomer-modified poly(HEMA-silica) nanoparticles [26] and to fabricate nanoparticle–polymer hybrid nanofibers via electrospinning [27].

Previously, our group [28] reported a convenient synthetic route to prepare transparent poly(acrylic-silica) hybrid materials with low volume shrinkage of 6–20% that lessened the above-mentioned problems. This methodology utilized commonly available sol–gel precursors such as tetraethyl orthosilicate (TEOS) and polar vinyl monomers such as 2-hydroxyethyl methacrylate (HEMA). Poly(HEMA-silica) hybrid materials were synthesized by three simultaneous reactions, namely: (1) hydrolysis and condensation of tetraethyl orthosilicate to form the silica phase, (2) condensation of the hydroxyl groups in silanol with those in HEMA to form HEMA–silica bonds, and (3) free radical polymerization of vinyl groups in HEMA-silica and unbounded HEMA to form the interconnecting poly(HEMA-silica) copolymers within the silica network. First, the hydrolysis and condensation reactions of TEOS (sol–gel reactions) were allowed to proceed in the presence of HEMA until the translucent mixture disappeared and a homogeneous solution resulted. The silanol groups on the silicate colloids or hydrolyzed TEOS then reacted with the OH group on HEMA to form the covalent linkage between the monomer and the inorganic silicate component. At this stage, the free radical initiator was dissolved in the solution and the reaction system was evacuated to remove the large amount of solvents present in the reaction medium. The resultant non-volatile liquid was then polymerized at increased temperature. The vinyl polymerization proceeded simultaneously with the sol–gel reactions to form the hybrid material with the organic–inorganic phases existing as a molecular-level interpenetrating network. Poly(HEMA) was chosen as the matrix polymer because the HEMA monomer is able to react with the silanol (SiOH) groups in the silicate colloids or hydrolyzed TEOS. This approach has also led to the exploration of new potential applications for poly(acrylic-silica) hybrids such as dental restoratives or adhesives and rigid, transparent polymer nanocomposites.

In the present work, we used the low volume shrinkage sol–gel synthesis route to fabricate monolithic samples of poly(HEMA-silica) hybrids with various silica contents. Our goal was to develop transparent organic–inorganic hybrid materials with enhanced resistance to abrasion and wear for use either as bulk polymer sheets or as a hard abrasion-resistant coating. Nanoindentation and microscratch measurements can be used as a tool for an accurate estimation of mechanical properties of organic–inorganic hybrids. A number of research groups have successfully introduced nanoindentation and microscratch techniques for their material characterization [29–34]. To our knowledge, no reports so far illustrated nanoindentation and scratch testing in poly(HEMA-silica) hybrid materials. Here for the first time we introduce both the unique methods in hybrid materials' characteristic measurements. In addition, the optical transmittance, thermal properties and N_2 adsorption–desorption characterization of these poly(HEMA-silica) hybrid materials were evaluated by using UV–vis spectrophotometer and thermal analysis methods (DSC, differential scanning calorimetry; TGA, thermogravimetric analysis; DMA, dynamic mechanical analysis) and BET (Brunauer–Emmett–Teller) method.

2. Experimental section

2.1. Materials

Tetraethyl orthosilicate (TEOS, Aldrich), 2-hydroxyethyl methacrylate (HEMA, Aldrich), tetrahydrofuran (THF, Aldrich) and hydrochloric acid (HCl, Fisher) were used as received.

Benzoyl peroxide (BPO, Aldrich) was recrystallized with ethyl alcohol before use.

2.1.1. Synthesis of the hybrid materials

In general, TEOS, HEMA, distilled water, HCl and THF were placed in a three-neck flask equipped with a condenser, a magnetic stirrer and a nitrogen gas inlet–outlet. In a typical procedure for the preparation of 25 wt% SiO_2 poly(HEMA-silica) hybrid material, 52.083 g (0.25 mol) of TEOS and 45.068 g (0.346 mol) of HEMA were dissolved in 36.055 g (0.50 mol) of THF at room temperature. Then, 18 g (1 mol) of distilled water and 1.250 g of 2 M HCl were added to the solution. Initially, the mixture was translucent and upon stirring for about 15 min, it became transparent at room temperature. The solution was refluxed at 70 °C for 2.5 h. After the solution cooled to room temperature, 0.042 g ($0.017\acute{}\ 10^{-3}$ mol) of benzoyl peroxide (BPO) was added to the solution and dissolved. The solvent (i.e., THF) and by-products from sol–gel process (i.e., ethanol and water) were removed via vacuum distillation at room temperature. The vacuum distillation was stopped when the residue in flask reached around 64 g without gelation, otherwise the gelation happened below this value. The resulting transparent solution was cast into cylindrical polyethylene molds (diameter: 0.8 in and depth: 2 in) and placed in an oven at 80 °C for 12 h to complete the polymerization.

2.1.2. Sample preparation

Cylindrical discs 0.25 in thickness were cut by electric saw and the disc surfaces were polished with 60, 180, and 600 grit sand papers successively. They were then polished with Lecloth and toothpaste (polishing agent) on a LECO polishing machine VP-160. A schematic of the cast cylinder along with the typical discs cut from the cylinder is shown in Fig. 1A. The nanoindentation and microscratch measurements were performed on the optically clear surface of polished discs and thus represent the bulk properties of as-cast hybrid samples.

2.2. Characterization and testing of poly(HEMA-silica) hybrids

2.2.1. Optical analysis

Optical transmittance of poly(HEMA-silica) hybrid materials in the visible region was measured with a S2000 Miniature Fiber Optic Spectrometer (Ocean Optics Inc., FL).

2.2.2. Thermal analysis

DSC, DMA, and TGA were used to determine the glass transition temperature and thermal stability of poly(HEMA-silica) hybrid polymers. Thermal stability measurements were made in air with a TA 100 TGA equipped with TQ 50 module. Characterization of glass transition was performed in nitrogen with a TA 100 DSC equipped with TQ 100 module. The samples used in TGA and DSC were initially dried at 60 °C in a vacuum oven for 60 h. After drying, the samples were ground into powder and sieved through a 250 mesh sieve.

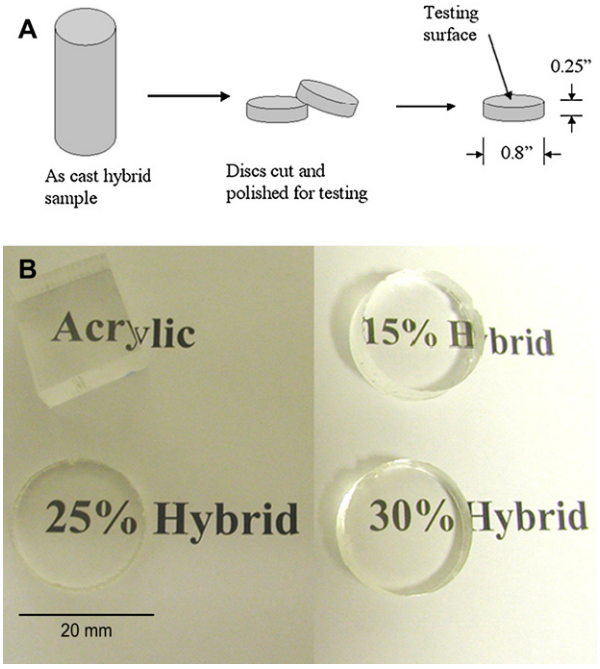

Fig. 1. (A) Schematic representation of the sample dimensions of the cast hybrid samples. (B) Pictures of polished poly(HEMA-silica) hybrid nanocomposite samples and Plexiglas® (PMMA) sample.

In a typical TGA test, the powder was first heated to 120 °C at a rate of 10 °C/min and then held at 120 °C for 10 min. After cooling to 40 °C, the powder sample was heated to 800 °C and the weight of the residue was measured at 750 °C. In a DSC experiment, the sample was heated from room temperature to 150 °C and then cooled to 0 °C; it was then re-heated to 200 °C. The heating and cooling rates were 10 °C/min in all instances. DMA was performed by using a Perkin–Elmer 7e DMA wherein the sample was heated from 20 to 180 °C at a rate of 2 °C/min. The test was performed at a fixed frequency of 1 Hz.

2.2.3. N_2 adsorption–desorption characterization

The poly(HEMA-silica) samples were ground and sieved through a 40 mesh sieve, then the powder was degassed overnight at 120 °C. The N_2 adsorption–desorption characterization was conducted by a Micromeritics ASAP 2010 analyzer (Micromeritics, Inc., Norcross, GA) at −196 °C (liquid nitrogen).

2.2.4. Nanoindentation

The modulus and hardness of the poly(HEMA-silica) nanocomposites were determined with the use of nanoindentation technique. The measurements were performed using Hysitron TriboIndenter with a Berkovich tip (nominal radius of 50 to 100 nm). The frame compliance and area function calibration of the tip were conducted with fused silica standard prior to the testing of hybrid materials. Samples were tested at a constant rate of 50 μN/s during loading and unloading. Three different loads of 500, 1000, and 2000 μN were used in the nanoindentation measurements.

The modulus and hardness of the samples were calculated from the unloading curve of the load–displacement plot. The hardness of the samples is given by:

$$H = \frac{P_{\max}}{A}$$

where A is the area function of the Berkovich indentor determined in the calibration experiments. The effective modulus of the samples was then calculated from the unloading stiffness (slope of the unloading curve) and using Oliver and Parr equation [35]:

$$S = \beta \frac{2}{\sqrt{\pi}} E_{\text{eff}} \sqrt{A}$$

where S is the unloading stiffness and E_{eff} is the sample elastic modulus.

2.2.5. Microscratch testing

Microscratch testing was performed with a Nano Scratch Tester (model: NSTX, CSM Instruments Inc.) with a diamond tip of radius 2 μm (indenter type: Rockwell). A progressive load scratch test was performed where the sample surface was scratched at a constant displacement rate traveling in the horizontal direction for a total length of 1 mm with load level increasing from 0 to 100 mN. The final depth of the scratch was approximately 10 μm.

3. Results and discussion

3.1. Synthesis of hybrid materials and physical appearance

The synthesis resulted in the fabrication of completely transparent hybrid materials with good dimensional stability and low volume shrinkage during polymerization. This clearly shows that our synthesis technique would allow for the fabrication of thick monolithic organic–inorganic samples by conventional cell casting, thus eliminating the drawbacks associated with sol–gel synthesis such as excessive shrinkage resulting from the need for removing the residual solvent. Moreover, because of the lower volume shrinkage during casting, the induced stresses are significantly reduced and thereby prevent crack formation during curing and post-cure annealing processes.

Fig. 1B shows the excellent optical transparency of polished poly(HEMA-silica) hybrid samples. A PlexiGlas® (poly(methyl methacrylate)) sample is also shown in Fig. 1B for comparison purposes. All poly(HEMA-silica) hybrid samples display excellent transmission, namely, 95% in the visible region and are comparable to the acrylic polymer. The fact that all the hybrid samples exhibit transparency equivalent to the unfilled poly(HEMA) suggests that no precipitation of silica occurred during the synthesis and that the size of the silica domains in these hybrid polymers should be below 400 nm and hence do not scatter visible light. This result is consistent with earlier poly(acrylic-silica) hybrids synthesized via a solvent-based sol–gel technique, indicating a molecular-level linking of silica and HEMA [36].

3.2. Thermal properties

DSC measurements performed on the hybrid polymers revealed that the poly(HEMA-silica) hybrid materials did not have a significant glass transition temperature (T_g) and the T_g of the baseline polymer, poly(HEMA), at about 102 °C (Fig. 2). This lack of observable transition in the poly(HEMA-silica) hybrid samples is most likely attributable to the influence of the crosslinking that occurs via cross-polymerization of the growing poly(HEMA) polymer chains with HEMA pendant groups on the silica structure formed by the condensation of HEMA with the silica. As such, the large-scale cooperative segmental motion of the polymer chains is restricted. The resolution of DSC is limited to the thermal conduction length in the order of 15–30 nm.

However, results of the DMA revealed that the glass transition was not completely suppressed in the hybrid samples and was strongly influenced by the amount of silica in the hybrid materials. The intensity of the tan δ peak in all the poly(HEMA-silica) hybrid polymers was reduced compared to the poly(HEMA), which was consistent with the restriction of polymer chain mobility observed in DMA (Fig. 3). The data of DMA, a more sensitive method, showed that at low silica contents (e.g., 15 wt%), there is a prominent tan δ peak. However, the transition temperature occurred at a much lower temperature than that of the poly(HEMA) (70 °C vs. 102 °C). Habsuda et al. [37] obtained the similar results in DSC and DMA measurements of the poly(HEMA-silica) system with SiO_2 content <10 wt% derived from HEMA and silicic acid. In our case, as the silica content was increased to 25 wt%, the tan δ peak became broad and further suppressed. In contrast, at 30 wt% silica of the sample exhibited a broadened T_g at about 100 °C. We postulated a mechanism for disrupting the poly(HEMA) polymer entanglements through the incorporation of the silica phase at low silica contents. The silica

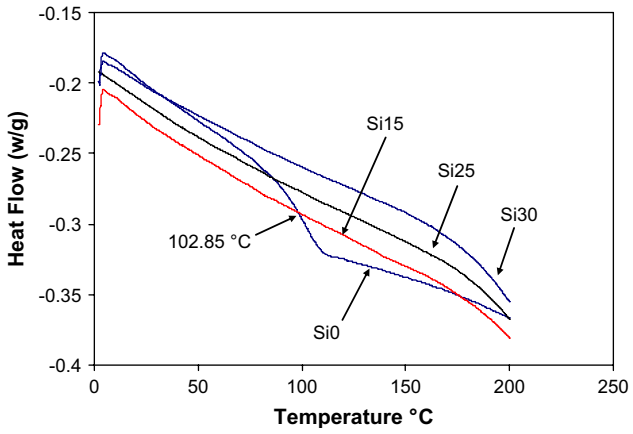

Fig. 2. DSC plots of samples recorded at a heating rate of 10 °C/min. Si0: poly(HEMA) as control; Si15: poly(HEMA-silica), 15 wt% SiO_2; Si25: poly(HEMA-silica), 25 wt% SiO_2; Si30: poly(HEMA-silica), 30 wt% SiO_2.

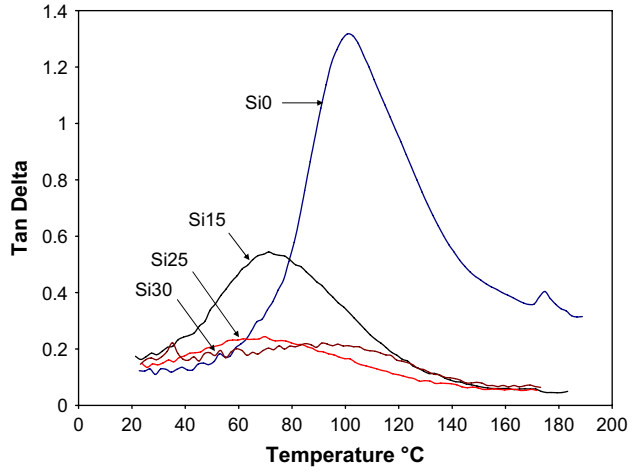

Fig. 3. Plots of tan δ against temperature in DMA measurements. Si0: poly(HEMA) as control; Si15: poly(HEMA-silica), 15 wt% SiO_2; Si25: poly(HEMA-silica), 25 wt% SiO_2; Si30: poly(HEMA-silica), 30 wt% SiO_2.

might function like "plasticizers" (particularly if the sol–gel reactions are incomplete), leading to lowered T_g values. When the silica content was further increased to 30 wt%, crosslinked silica might have formed (i.e., above the network threshold). This would result in the observed increase in T_g value at high silica contents (e.g., 30 wt%).

In the DMA data (Fig. 4), we also saw a drastic increase of the rubbery plateau (or post-T_g) modulus of poly(HEMA-silica) with increasing silica content. The 30 wt% silica sample exhibited an almost two-order magnitude higher storage modulus than that of the poly(HEMA), further indicating the formation of a glass-like, crosslinked poly(HEMA-silica) network. Moreover, this dramatic increase in the storage modulus could only be due to molecular-level reinforcement of the entangled polymer structure by an interpenetrating network of inorganic silica.

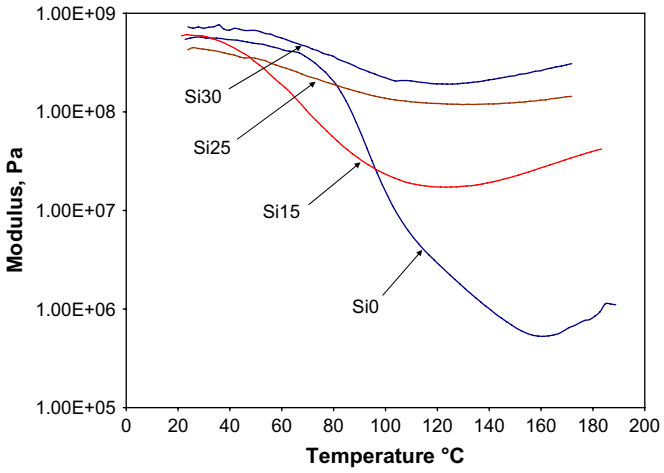

Fig. 4. Storage modulus as a function of temperature in DMA measurements at a fixed frequency of 1 Hz of storage modulus. Si0: poly(HEMA) as control; Si15: poly(HEMA-silica), 15 wt% SiO_2; Si25: poly(HEMA-silica), 25 wt% SiO_2; Si30: poly(HEMA-silica), 30 wt% SiO_2.

3.3. N_2 adsorption–desorption characterization of poly(HEMA-silica)

The adsorption–desorption isotherm shows that BET surface area is 0.83 m^2/g, which is typical of nonporous materials. The pore volume was approximately 3×10^{-4} cm^3/g showing that the poly(HEMA-silica) has no internal porosity.

For pure SiO_2 gels prepared by the sol–gel method, surface areas in excess of 200 m^2/g [16] have been observed with pore volumes larger than 0.1 cm^3/g. The pores were formed during the evaporation of volatile by-products from the gel. However, in case of our poly(HEMA-silica), the byproduct is removed by vacuum evaporation while the material is still in the sol state. HEMA monomers would enter and polymerize inside pores that would render the hybrid product essentially nonporous.

3.4. Thermogravimetric analysis

The thermal stability of any crosslinked polymer is generally greater than a linear polymer. The poly(HEMA-silica) hybrid polymers showed improved thermal stability as observed by a reduction in mass loss rate from the TGA measurements in air (Fig. 5). This is expected as the polymer phase present within the silica network is shielded from the high temperature environment and thus, it would be expected to have a higher thermal stability. The hypothesis of the formation of a percolated poly(HEMA-silica) network is further evidenced by the silica residues remaining at the end of the TGA experiments. The exact silica content was determined from the weight of the residue at 750 °C, and these values were in excellent agreement with those calculated from stoichiometry of the starting materials.

3.5. Modulus and hardness of poly(HEMA-silica) hybrids

In this study, nanoindentation was for the first time used to measure the hardness and modulus of the poly(HEMA-silica) hybrid samples. Indentation experiments were performed at three different loads, namely, 500, 1000, and 2000 μN. In

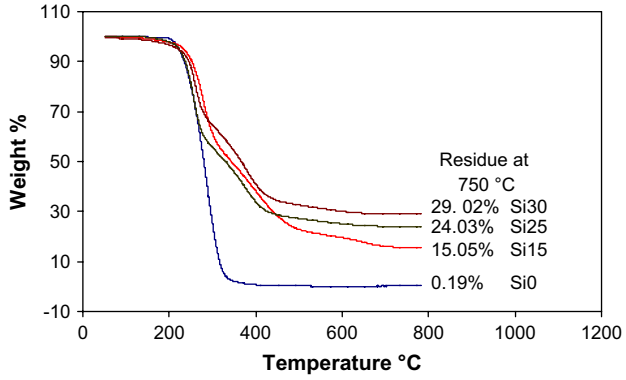

Fig. 5. TGA curves of the hybrid samples and control sample recorded at a heating rate of 10 °C/min in air.

Table 1
Modulus and hardness of poly(HEMA-silica) hybrids measured by using nanoindentation at three different loads of 500, 1000 and 2000 μN

Property	Modulus, GPa			Hardness, GPa		
Load, μN	500	1000	2000	500	1000	2000
PHEMA (control)	4.45 (0.363)	4.40 (0.423)	4.33 (0.174)	0.214 (0.033)	0.212 (0.030)	0.195 (0.015)
PHEMA-silica (15 wt% SiO_2)	4.34 (0.205)	4.13 (0.092)	4.24 (0.116)	0.265 (0.018)	0.236 (0.010)	0.220 (0.011)
PHEMA-silica (25 wt% SiO_2)	4.96 (0.181)	4.84 (0.152)	4.49 (0.14)	0.31 (0.017)	0.277 (0.016)	0.254 (0.007)
PHEMA-silica (30 wt% SiO_2)	6.19 (0.353)	5.76 (0.166)	5.59 (0.169)	0.376 (0.046)	0.336 (0.009)	0.306 (0.011)

Numbers in parentheses represent standard deviation.

each case, the sample modulus and hardness were determined from the unloading curve. The values of modulus and hardness of the poly(HEMA) and hybrids measured at these loads are tabulated in Table 1. Typical loading and unloading curves for 1000 μN are presented in Fig. 6. At any constant load, the penetration depth of the indenter into the sample decreased with increasing silica content, clearly indicating an increase in the hardness of poly(HEMA-silica) hybrids upon addition of the silica. A percolation threshold appears at about 20–25 wt% of silica, and this is consistent with the dependence of rubbery plateau modulus enhancement on silica network formation observed in DMA.

3.6. Microscratch testing

Scratch resistance of these poly(HEMA-silica) hybrids was evaluated for the first time by using microscratch measurements. The poly(HEMA) sample exhibited a tearing mode of failure near the scratch edge, which was accompanied with material "pile-up" as shown in Fig. 7A, which is typical for polymeric materials. On the other hand, all poly(HEMA-silica) hybrids (Fig. 7B) do not show the same tearing upon scratching. Rather, the hybrid samples failed by cracking indicative of glassy type of failure. This is presumably a result of shear deformation of materials upon scratching. The number of cracks formed along the length of the scratch decreased with an increase in the silica content, suggesting that the incorporation of silica in the poly(HEMA) matrix leads to poly(HEMA-silica) hybrids with significantly higher resistance to scratch and abrasion.

In addition to the studies of failure mechanisms, the scratch-resistant properties as a function of silica loading for these poly(HEMA-silica) hybrid materials were also investigated. The force associated with the initial failure was defined as the load at which the initial crack or tear occurred. We determined this by locating the first visible crack or tear along the scratch from the microscopy images. Then, the corresponding force value was calculated for that tear or crack from the force–displacement data for the given constant loading rate scratch experiment. Table 2 summarizes the values of initial failure load as well as the mode of failure from microscratch measurements. The initial failure load increased

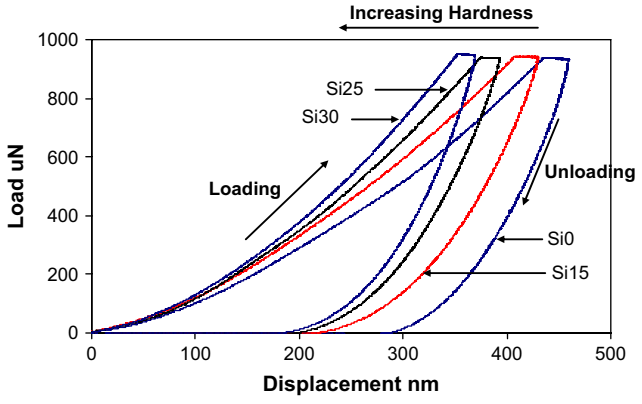

Fig. 6. Load vs. displacement curves upon nanoindentation of the sample at 1000 μN load. Poly(HEMA-silica) hybrid samples showed increasing modulus and hardness with silica content compared to a control sample with no silica. Si0: poly(HEMA) as control; Si15: poly(HEMA-silica), 15 wt% SiO_2; Si25: poly(HEMA-silica), 25 wt% SiO_2; Si30: poly(HEMA-silica), 30 wt% SiO_2.

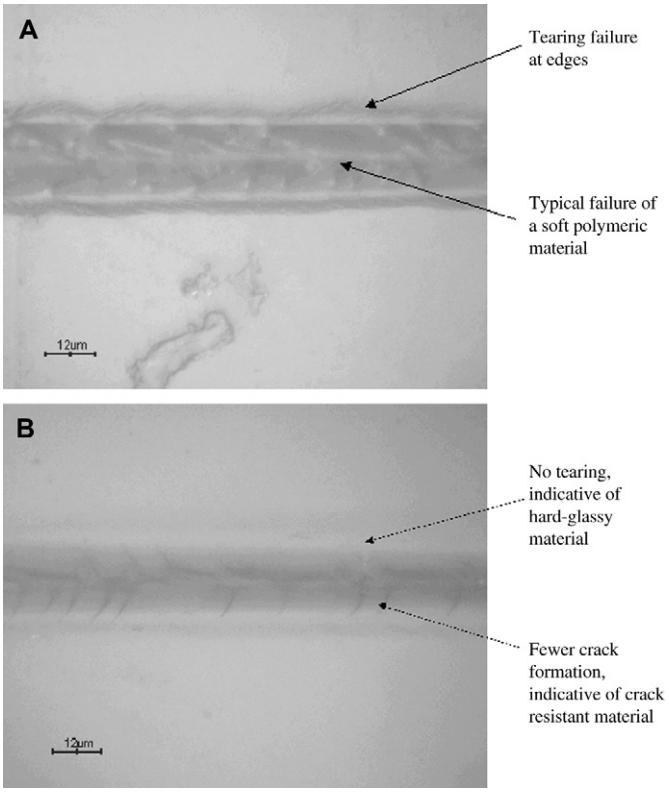

Fig. 7. (A) Deformation and cracking of control sample poly(HEMA) under progressive load scratching. The sample shows typical failure of soft, low modulus polymeric materials. (B) Deformation and cracking of Si30, a hybrid containing 30 wt% of silica. Failure mode has changed from a soft polymeric material to a hard-glassy material due to the addition of silica.

Table 2
Failure mode and failure initiation force as observed using microscratch testing

Sample	Mode of failure	Load at first crack, mN
PHEMA (control)	Tearing	12
PHEMA-silica (15 wt% silica)	Cracking	28
PHEMA-silica (25 wt% silica)	Cracking	47
PHEMA-silica (30 wt% silica)	Cracking	68

five-fold for the 30 wt% silica samples as compared with the poly(HEMA), clearly indicating the effectiveness of poly(silica-HEMA) hybrids to protect against scratch hazards. This is consistent with the hardness and modulus results obtained from nanoindentation.

4. Summary and conclusions

Poly(HEMA-silica) hybrids with low volume shrinkage were synthesized via sol–gel reactions in conjunction with free radical polymerization of vinyl groups in HEMA. Results clearly demonstrate that this approach would allow for the fabrication of thick monolithic organic–inorganic nanocomposites by conventional cell casting without the major concerns of dimensional stability and shrinkage-induced crack formation. All the hybrid materials displayed excellent optical transmission, namely, ~95% in the visible region which indicates the formation of a molecular-level hybrid material with the size of the silicate domains in these poly(HEMA-silica) hybrids being well below the wavelength of visible light. As expected, the hardness and modulus of poly(HEMA-silica) hybrids increased with increasing silica content. A percolation threshold of about 20–25 wt% of silica was observed, above which, there was a drastic increase in hardness and modulus over the pure poly(HEMA). The 30 wt% silica hybrid exhibited a 60% increase in hardness and a 33% increase in modulus. Similarly, the rubbery plateau modulus of poly(HEMA-silica) hybrids obtained from DMA increased significantly with respect to silica loading, which supports our conclusion of molecular-level reinforcement of the entangled polymer structure by an interpenetrating network of inorganic silica. Microscratch measurements revealed different modes of failure associated with deformation of poly(HEMA) and poly(HEMA-silica) hybrids. The poly(HEMA) exhibited a tearing failure at the scratch edge and material pile-up indicative of poor scratch resistance. In contrast, all the poly(HEMA-silica) hybrids showed a more glassy type of failure. The scratch resistance performance determined from the initial load value associated with the first tearing or crack failure increased with increasing silica content. The 30 wt% silica hybrid displayed a five-fold increase in the resistance to microscratch over poly(HEMA).

Through this work, we showed a facile method to prepare low shrinkage sol–gel hybrid materials and the property enhancements associated with the molecular-level interpenetrating poly(acrylic-silica) network. Increase in hardness, modulus, and scratch resistance of the hybrid materials and the ability to make samples with low shrinkage during cure shows promise of these materials for applications either as bulk polymer sheets or as hard abrasion-resistant coatings.

Acknowledgments

This work was supported by the U.S. Army Research Laboratory (Contract No. W911QX-04-C-0041) and by the National Institutes of Health (Grant No. DE09848). We thank Dr. Alan Schwartzman, NanoMechanical Technology Laboratory at the Massachusetts Institute of Technology, for assisting with the Nanoindentation testing and Dr. Nicholas Randall, CSM Instruments, for assisting with the microscratch analysis.

References

[1] Mackenzie JD, Ulrich DR. Ultrastructure processing of advanced ceramics. New York, NY: Wiley; 1988.
[2] Brinker CJ, Scherer GW. In: Sol–gel science: the physics and chemistry of sol–gel processing. San Diego, CA: Academic Press; 1990.
[3] Wilkes GL, Huang H, Glaser RH. In: Ziegler JM, Fearon FWG, editors. Silicon-based polymer science. Advances in chemistry series 224. Washington, DC: American Chemical Society; 1990. p. 207–26.
[4] Novak BM. Adv Mater 1993;2:337–9.
[5] Mark JE, Lee CY-C, Bianconi PA, editors. Hybrid organic–inorganic composites. ACS Symposium Series 585. Washington, DC: American Chemical Society; 1995.
[6] Wen J, Wilkes GL. Chem Mater 1996;8:1667–81.
[7] Judenstein P, Sanchez C. J Mater Chem 1996;6:511–25.
[8] Costa RC, Vasconcelos WL. J Non-Cryst Solids 2002;304:84–91.
[9] Schottner G. Chem Mater 2001;13:3422–35.
[10] Wei Y. In: Buschow KHJ, Cahn RW, Flemings MC, Hschner B, Kramer EJ, Mahajan S, editors. Encyclopedia of materials: science and technology. Oxford, UK: Elsevier Science Ltd.; 2001. p. 7594–605.
[11] Sanchez C, Julián B, Belleville P, Popall M. J Mater Chem 2005;(35–36):3559–92.
[12] Ogoshi T, Miyake J, Chuj Y. Macromolecules 2005;38:4425–31.
[13] Ogoshi T, Chujo Y. Compos Interfaces 2005;11:539–66.
[14] Novak BM, Davies C. Macromolecules 1991;24:5481.
[15] Yeh JM, Weng CJ, Huang KY, Lin CC. J Appl Polym Sci 2006;101:1151–9.
[16] Liu W, Zhang Y, Wang C. Inorg Mater 2006;42:641–6.
[17] Hueh E, Stieger M, Klee JE, Frey H, Huelhaupt R. J Polym Sci 2001;39:4274–82.
[18] Cho Y, Shin C, Kim N, Yusuke K. Abstracts of papers, 229th ACS National Meeting. San Diego, CA, United States; March 13–17, 2005.
[19] Rao AV, Pajonk GM. J Non-Cryst Solids 2001;285:202–9.
[20] Novak BM, Ellsworth MW, Verrier C. In: Mark JE, Lee YC, Bianconi PA, editors. Hybrid organic–inorganic composites. ACS Symposium Series 585. Washington, DC: Americam Chemical Society; 1995. p. 86–96 [chapter 8].
[21] Bosch P, Monte FD, Levy DJ. J Polym Sci 1996;34:3289–96.
[22] Hajji P, David L, Gerard JF, Pascault JP, Vigier G. J Polym Sci 1999;37:3172.
[23] Hajji P, Vigier G, Pascault JM. Elf-Atochem JP. Quai Louis Aulagne, Saint-Fons, France. Verre (Versailles), vol. 6; 2000. p. 9–20.
[24] Lin D, Chen C, Chang C, Su Y, Cheng L. J Polym Res 2002;9:115–8.
[25] Huang S, Chin W, Yang WP. J Polym Sci Part B Polym Phys 2004;42:3476–86.
[26] Wei Y, Feng Q, Cheng S, Li S. Polym Mater Sci Eng 2003;89:311.
[27] Sun Z, Li S, Patel A, Wang C, Wei Y. Abstracts of papers, 228th ACS National Meeting. Philadelphia, PA, United States; August 22–26, 2004.
[28] Wei Y, Jin DL, Yang CC, Wei G. J Sol Gel Sci Technol 1996;7:191–201.

[29] Soloukhin VA, Posthumus W. Polymer 2002;43:6169–81.
[30] Mammeri F, Rozes L, Sanchez C, Bourhis EL. J Sol Gel Sci Technol 2003;26:413–7.
[31] Mammeri F, Bourhis EL. J Eur Ceram Soc 2006;26:259–66.
[32] Zhang X, Hu L, Sun D. Acta Mater 2006;54:5469–75.
[33] Wen H, Wang X, Li L. J Appl Phys 2006;100:084315.
[34] Wong M, Lim GT, Moyse A, Reddy JN, Sue H-J. Wear 2004;256:1214–27.
[35] Oliver WC, Pharr GM. J Mater Res 1992;7:1564–83.
[36] Wei Y, Jin D, Xu J, Baran G, Qiu KY. Polym Adv Technol 2001;12:361–8.
[37] Habsuda J, Simon GP, Cheng DG, Hewitt DG, Diggins DR, Toh H. Polymer 2002;43:4627–38.